BAYESIAN ORBIT COMPUTATION TOOLS FOR OBJECTS ON GEOCENTRIC ORBITS

J. Virtanen[(1)], M. Granvik[(2)], K. Muinonen[(1)(2)], and D. Oszkiewicz[(3)]

[(1)] *Finnish Geodetic Institute, Masala, FINLAND, Email: Jenni.Virtanen@fgi.fi*
[(2)] *University of Helsinki, Helsinki, FINLAND*
[(3)] *Adam Mickiewicz University, Poznan, POLAND*

ABSTRACT

We consider the space-debris orbital inversion problem via the concept of Bayesian inference. The methodology has been put forward for the orbital analysis of solar-system small bodies in early 1990's [7] and results in a full solution of the statistical inverse problem given in terms of a posteriori probability density function (PDF) for the orbital parameters. We demonstrate the applicability of our statistical orbital analysis software to Earth-orbiting objects, both using well-established Monte Carlo (MC) techniques (for a review, see e.g. [13] as well as recently developed Markov-chain MC (MCMC) techniques (e.g., [9]). In particular, we exploit the novel virtual-observation MCMC method [8], which is based on the characterization of the phase-space volume of orbital solutions before the actual MCMC sampling. Our statistical methods and the resulting PDFs immediately enable probabilistic impact predictions to be carried out. Furthermore, this can be readily done also for very sparse data sets and data sets of poor quality - providing that some a priori information on the observational uncertainty is available. For asteroids, impact probabilities with the Earth from the discovery night onwards have been provided, e.g., by [11] and [10], the latter study includes the sampling of the observational-error standard deviation as a random variable.

Key words: orbits; statistical inversion; Bayesian inference.

1. INTRODUCTION

We consider the space-debris orbital inversion problem via the concept of Bayesian inference. The methodology has been put forward for the orbital analysis of solar-system small bodies in early 1990's [7]. In the Bayesian formalism the parameters to be solved for are treated as random variables and the entire orbital solution, including uncertainty information, is contained in the resulting posterior orbital-element distribution. Furthermore, all 6 dimensions are treated rigorously, that is, without predefining the shape (such as Gaussian) of any parts of the posterior distribution.

Several Bayesian methods for asteroid orbit computation have been developed during the last two decades and the latest developments, with particular application to ESA's Gaia mission, are summarized in [8]. These include well-established Monte Carlo (MC) techniques, such as statistical ranging, as well as recently developed Markov-chain MC (MCMC) techniques. In particular, we exploit the novel virtual-observation MCMC method [8], which is based on the characterization of the phase-space volume of orbital solutions before the actual MCMC sampling. All Bayesian orbit-computation methods that have been developed for asteroids are included in the open-source package OpenOrb which is covered by a GNU GPL v3 license [3]. OpenOrb is widely used in the asteroid community, e.g., as a part of the Pan-STARRS1 Moving Object Processing System and the Canadian NEOSSat mission launched on Feb 25, 2013.

2. STATISTICAL INVERSION PROBLEM

In orbit computation, the general *observation equation* describes the relation between observed positions and computed positions:

$$\boldsymbol{\psi} = \boldsymbol{\Psi}(\boldsymbol{P}) + \boldsymbol{\varepsilon} + \boldsymbol{\nu} \,. \qquad (1)$$

The vector $\boldsymbol{\psi}$ contains the observed positions which are typically given as Right Ascension (RA) and Declination (Dec) pairs for the observation dates. $\boldsymbol{P}$ contains the six orbital elements—such as the Cartesian position and velocity in three-dimensional space—at a specified epoch t_0. The nonlinear function $\boldsymbol{\Psi}(\boldsymbol{P})$ gives the light-time-corrected topocentric positions computed from the orbital elements for the observation dates. $\boldsymbol{\varepsilon}$ and $\boldsymbol{\nu}$ describe the random and systematic errors, respectively. For most modern asteroid applications, the systematic error is small enough to be incorporated into the typically much larger random error. In what follows, the systematic error is assumed negligible, that is, $\boldsymbol{\nu} \sim 0$.

The problem of computing positions $\boldsymbol{\Psi}$, that is, ephemerides, based on a set of orbital elements $\boldsymbol{P}$ is called the *direct problem* of orbit computation. The *inverse problem* is to find the orbital elements $\boldsymbol{P}$ given a set of observed positions $\boldsymbol{\psi}$. In the statistical inverse theory, the (a posteriori) orbital-element probability-density function (PDF) $p_{\rm p}$ is proportional to the a priori ($p_{\rm pr}$) and observational error (p_ϵ) PDFs:

$$p_{\rm p}(\boldsymbol{P}) = C\, p_{\rm pr}(\boldsymbol{P})\, p_\epsilon(\Delta\boldsymbol{\psi}(\boldsymbol{P}))\,. \tag{2}$$

$C = (\int p(\mathbf{P},\boldsymbol{\psi})\, d\mathbf{P})^{-1}$ is the normalization constant, where the joint PDF is $p(\mathbf{P},\boldsymbol{\psi}) = p_{\rm pr}(\boldsymbol{P})\, p_\epsilon(\Delta\boldsymbol{\psi}(\boldsymbol{P}))$. Whereas p_ϵ is evaluated for the $O-C$ residuals $\Delta\boldsymbol{\psi}(\boldsymbol{P})$ and is usually assumed to be Gaussian due to the central limit theorem, [7] experimented with non-Gaussian noise statistics. They concluded that a significant improvement in the results, outweighing the more cumbersome analysis, could not be obtained.

To secure the invariance of the orbital-element PDF $p_{\rm p}$ in transformations between different types of orbital elements (e.g., from Cartesian to Keplerian), the analysis can be regularized by Jeffreys' a priori PDF $p_{\rm pr,J}$ [6]:

$$\begin{aligned} p_{\rm pr,J}(\boldsymbol{P}) &\propto \sqrt{\det\Sigma^{-1}(\boldsymbol{P})}, \\ \Sigma^{-1}(\boldsymbol{P}) &= \Phi(\boldsymbol{P})^T\Lambda^{-1}\Phi(\boldsymbol{P}), \end{aligned} \tag{3}$$

where Σ^{-1} is the information matrix evaluated for the local orbital elements $\boldsymbol{P}$, Φ contains the partial derivatives of the observed coordinates (usually RA and Dec) with respect to the orbital elements, and Λ is the covariance matrix for the observational errors. Finally, the a posteriori orbital-element PDF is given by

$$\begin{aligned} p_{\rm p}(\boldsymbol{P}) &\propto \sqrt{\det\Sigma^{-1}(\boldsymbol{P})}\ \exp\left[-\frac{1}{2}\chi^2(\boldsymbol{P})\right], \\ \chi^2(\boldsymbol{P}) &= (\Delta\boldsymbol{\psi}(\boldsymbol{P}))^T\Lambda^{-1}\Delta\boldsymbol{\psi}(\boldsymbol{P}). \end{aligned} \tag{4}$$

The a posteriori PDF $p_{\rm p}$ can also include an informative a priori PDF $p_{\rm pr,inf}$, which is included as a separate factor in Eq. (4)

$$p_{\rm p}(\boldsymbol{P}) \propto p_{\rm pr,inf}(\boldsymbol{P})\sqrt{\det\Sigma^{-1}(\boldsymbol{P})}\ \exp\left[-\frac{1}{2}\chi^2(\boldsymbol{P})\right]\,. \tag{5}$$

The informative a priori PDF can, for example, be used to set constraints on the a posteriori PDF, or to combine inversion results obtained for different observation sets (an orbital-element PDF computed from radar observations as an a priori PDF for the inverse problem of optical astrometry, or vice versa).

The orbital-element PDF $p_{\rm p}$ obtained can be transformed to the joint PDF of any other parameter set ($\boldsymbol{F}(\boldsymbol{P}) = (F_1(\boldsymbol{P}),\ldots,F_K(\boldsymbol{P}))^T$) by the following relation given in [7]:

$$p(\boldsymbol{F}) = \int d\boldsymbol{P}\ p_{\rm p}(\boldsymbol{P})\ \delta_{\rm D}(F_1 - F_1(\boldsymbol{P}))\ldots\delta_{\rm D}(F_K - F_K(\boldsymbol{P}))\,, \tag{6}$$

where $\delta_{\rm D}$ is Dirac's delta function. For example, Eq. (6) can be used to transform the orbital-element PDF from one set of elements to another (e.g., from Cartesian elements to Keplerian elements), or to propagate the orbital-element PDF to the ephemerides PDF.

3. NUMERICAL ALGORITHMS

In the following, we will describe some of the numerical algorithms which can be used to solve the orbital element PDF. We focus on the methods most useful for the short-arc problem, where the observations are either sparse and/or limited in their amount. For asteroids, this is typically the case after the discovery. For space debris, it is more a question of re-discovery, which may happen recurrently after several revolutions, if the separate data sets cannot be linked to belong to the same object, thus leading to cataloguing (see 4. Discussion).

All of the algorithms make use of Monte Carlo (MC) sampling of the phase-space volume of acceptable orbits:

- There is no need for any a priori assumption about the mathematical form of the a posteriori probability density, e.g. Gaussian. In fact, for short-arcs it is typical that solution space exhibits varying morphologies, which can be highly non-Gaussian.
- Information on observational errors can be readily incorporated, see Eq. (2).
- A priori information can be readily incorporated, see Eq. (5).
- The PDF computation can be carried out in different orbital parameters, e.g. Keplerian or Cartesian.

MC (Statistical) Ranging. The starting motivation for the Ranging algorithm [12] is to obtain a solution even with a minimum number of observations. This is accomplished by assuming six observational parameters, the minimum needed to solve for the six orbital parameters. This corresponds to sampling the orbital-element PDF in the phase-space of the observations, a natural choice, since the orbital solution space is known to be highly complex for short arcs and thus difficult to sample directly. The first four parameters are two sets of angular coordinates, obtained from optical observations, usually the first and the last are chosen, in case more than two observations are available. Two more parameters are obtained by assigning values for the topocentric distance for the two observation dates chosen. By combining these topocentric positions with the heliocentric locations of the observatory at the observation dates, two heliocentric positions equaling six constants of integration are known. These positions can then, in turn, be converted to orbital elements using either a two-body or an n-body solution to the two-point boundary-value problem.

The actual MC sampling goes as follows:

- Random angular deviations ($\Delta\alpha'_{\mathrm{A}}$, $\Delta\delta'_{\mathrm{A}}$, $\Delta\alpha'_{\mathrm{B}}$, $\Delta\delta'_{\mathrm{B}}$) are used to obtain a new set of angular coordinates, mimicking the observational errors in RA and Dec observations
- A topocentric distance ($\rho'_{\mathrm{A}} = \rho_{\mathrm{A},j} + \Delta\rho'_{\mathrm{A}}$) is randomly assigned for the first observation date and another random value is assigned for the difference between the topocentric distances at the two chosen observation dates ($\Delta\rho'_{\mathrm{AB}} = \Delta\rho_{\mathrm{AB},j} + \Delta(\Delta\rho'_{\mathrm{AB}})$). (This is because the two distance are highly correlated for close-by observations. Alternatively, separate random values for the distances can also be assigned.)
- Each candidate set of orbital element computed from the above positions is tested against the entire set of available observations, first, by using a $\Delta\chi^2$ criterion, and second by using cut-offs for the maximum observational residuals accepted (e.g. 3σ).
- Finally, the procedure is repeated until an predefined number of sample orbits have been accepted.

MCMC Ranging. In the Markov-Chain Monte Carlo (MCMC) version of Ranging [9], the MC random sampling above is replaced by guided sampling in terms of proposal densities: The Metropolis-Hasting (M-H) acceptance ratio for the proposed orbit is

$$a_r = \frac{p_p(\boldsymbol{P}')J_j}{p_p(\boldsymbol{P}_j)J'}\,, \tag{7}$$

where $\boldsymbol{P}_j$ and $\boldsymbol{P}'$ denote the current and proposed orbital elements in a Markov chain, and $J_j = \left|\frac{\partial \boldsymbol{Q}_j}{\partial \boldsymbol{P}_j}\right|$ and $J' = \left|\frac{\partial \boldsymbol{Q}'}{\partial \boldsymbol{P}'}\right|$ are the Jacobians between spherical coordinates and orbital elements (see e.g. [9] for details). The proposed elements $\boldsymbol{P}'$ are accepted ($\boldsymbol{P}_{j+1} = \boldsymbol{P}'$) with a probability $\min(1, a_r)$. If the proposed elements $\boldsymbol{P}'$ are not accepted then $\boldsymbol{P}_{j+1} = \boldsymbol{P}_j$. A Markov chain is thus essentially a sequence of random numbers that follow an arbitrarily complicated distribution. Note that for mapping multi-modal distributions, multiple Markov chains can be utilized. Note also that the convergence of the algorithm should be closely monitored with proper diagnostics (see [10]), and the orbital solutions obtained in the "burn-in" phase of MCMC should be excluded from the final a posteriori PDF.

Virtual-observation MCMC. When the observational arc grows longer and orbital-element PDF more confined, the above Ranging algorithms can be expected to slow down. To overcome this, another MCMC algorithm has been put forward by [8], which abandons the observation-space sampling and suggests to use a two-fold orbital-element sampling approach as follows. In the first part, the phase-space is characterized by N_V sets of virtual orbital elements, obtained by creating virtual observation sets

$$\boldsymbol{\psi}_{\mathrm{v}} = \boldsymbol{\psi} + \boldsymbol{\epsilon}_{\mathrm{v}}. \tag{8}$$

and minimizing

$$\chi^2_{\mathrm{v}}(\boldsymbol{P}) = (\boldsymbol{\psi}_{\mathrm{v}} - \boldsymbol{\Psi}(\boldsymbol{P}))^{\mathrm{T}}(\Lambda + \Lambda_{\mathrm{v}})^{-1}(\boldsymbol{\psi}_{\mathrm{v}} - \boldsymbol{\Psi}(\boldsymbol{P}))\,, \tag{9}$$

where the sum $\Lambda + \Lambda_{\mathrm{v}}$ reflects the presence of both real and virtual astrometric noise.

In the second part of the algorithm, we utilize the N_{v} virtual orbital solutions obtained in the first part in an M-H sampling by using the difference between two randomly chosen sets of virtual orbital elements as a symmetric proposal:

$$\Delta\boldsymbol{P}^{(jk)} = \boldsymbol{P}^{(j)}_{\mathrm{v}} - \boldsymbol{P}^{(k)}_{\mathrm{v}}, j,k = 1,2,3\ldots,N_{\mathrm{v}}; j \neq k\,. \tag{10}$$

These difference guide the sampling in the phase space and make it possible for the Markov chain to perform "jumps" from one phase-space region to another, efficiently mapping any nonlinearities in the a posteriori PDF.

Due to the symmetry of the proposal, the M-H acceptance ratio (7) reduces to

$$a_r = \frac{p_p(\boldsymbol{P}')}{p_p(\boldsymbol{P}_j)}\,. \tag{11}$$

4. DISCUSSION

To test the MCMC methods described in the previous chapter for geocentric orbits, we have applied the algorithms to the near-Earth object 2006 RH_{120}, so far the only discovered natural Earth satellite (NES; see [4], [5]). The few-meter-diameter asteroid was captured in 2006 and was observed for about a year, which it spent orbiting the Earth before it was ejected from the Earth-Moon system. Figure 1 shows the acceptable values of the geocentric distance at the discovery moment, while Figure 2 portrays the evolution of orbital uncertainties with increasing observational data.

According to [5], for all simulated NESs, after less than one day (or two subsequent nights of observations) all acceptable orbits are bound to the Earth at the observational

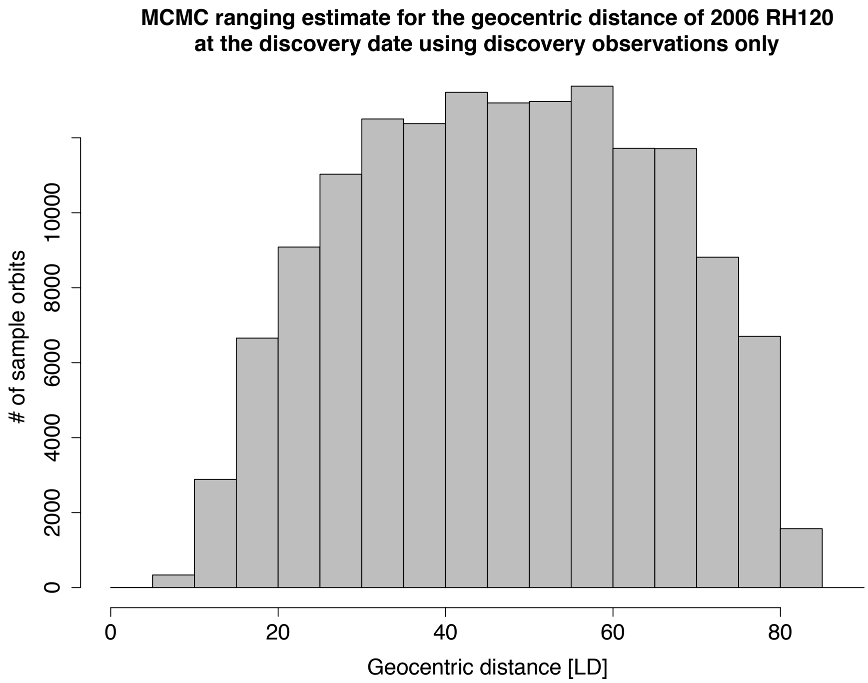

Figure 1. The distribution of geocentric distance at epoch 2006-09-14TT for 2006 RH_{120}.

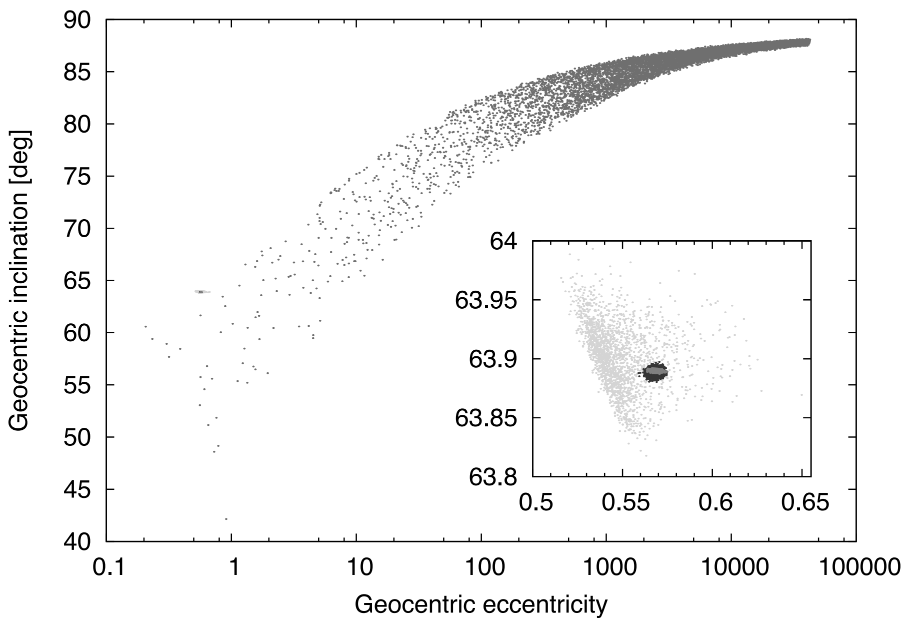

Figure 2. The distribution of geocentric eccentricity $e_{\oplus}$ and inclination $i_{\oplus}$ for the epoch 2006-09-14TT dramatically converges as a function of the observational timespan. The widest distribution covers a timespan of about 1.5 hours and includes all seven observations from the discovery telescope (Catalina Sky Survey's Mt. Bigelow station) only. The second distribution (close-up in the small frame) adds two observations from the Catalina Sky Survey's Siding Spring station and extends the observational timespan to about 7.5 hours. The third and fourth distributions are based on 12 and 26 observations spanning 25 and 56.2 hours, respectively. (Figure from [5])

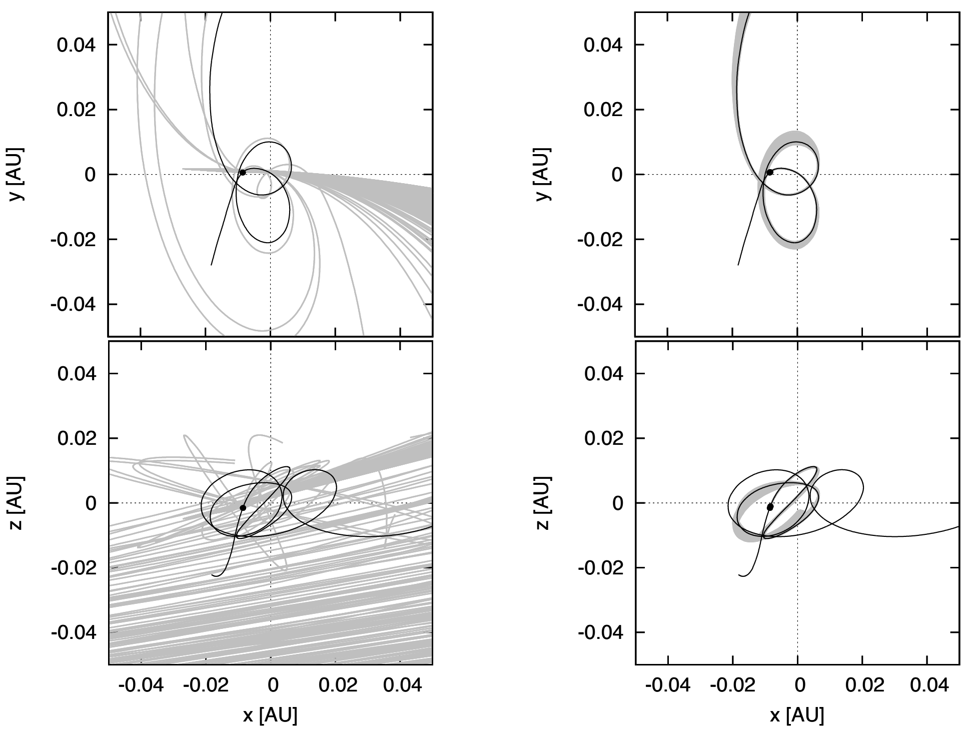

Figure 3. The evolution of the orbital uncertainty for a synthetic NES as a function of an increasing observational timespan and number of observations; (left) 3 detections during one hour, (right) 6 detections during 25 hours. The black line shows the true orbit in the XY and XZ planes in an ecliptic coordinate system that is co-rotating with the Sun so that the Earth is always in the center (0,0,0) and the Sun is always at about (1,0,0). The gray shaded area shows the extent of all acceptable orbits and the black dots mark the locations of the synthetic NES at the observation dates. All orbits have been followed for 500 days into the future starting from the inversion epoch and cut-offs based on, e.g., maximum geocentric distance are not used. (Figure from [5])

mid-epoch (see Fig. 3 for an example). This implies that the rapid convergence of the orbital solution seen in the case of 2006 RH_{120} is typical for all NESs. Less than a week of astrometry is required to obtain an accurate-enough orbit that can be utilized for planning detailed follow-up observations or an initial trajectory for a space mission.

Our statistical methods and the resulting orbital element PDFs immediately enable probabilistic analysis for space debris, such as population studies or impact predictions to be carried out. Furthermore, this can be readily done also for very sparse data sets and data sets of poor quality - providing that some a priori information on the observational uncertainty is available. To carry out population studies, a catalogue of individual space debris objects is needed, which in turn would require linking of individual space debris detections to specific objects. This is a demanding task and currently only around 16,000 objects have been catalogued. Efficient numerical methods developed for linking of asteroid observations ([1] and [2]) can be applied to space debris to improve the situation. In a similar manner, impact probabilities with the Earth can be estimated for individual space debris objects, as has been done for asteroids from the discovery night onwards, e.g., by [11] and [10], the latter study includes the sampling of the observational-error standard deviation as a random variable.

Regarding the orbit-computation algorithms, several improvements are due before fully applying them to lower-orbiting objects. In particular, we need to implement high-order terms of the Earth's gravitational potential as well as non-gravitational forces, such as the atmospheric drag and solar radiation pressure. Also, the use of more efficient, e.g. analytical algorithms for orbit propagation is a subject of further studies.

REFERENCES

1. Granvik, M., and K. Muinonen (2005). Asteroid identification at discovery, Icarus, vol. 179, pp. 109-127.
2. Granvik, M., and K. Muinonen (2008). Asteroid identification over apparitions, Icarus, vol. 198, pp. 130-137.
3. Granvik, M., et al. (2009). OpenOrb: Open-source asteroid-orbit-computation software including statistical ranging. *Meteoritics & Planetary Science* 44(12), 1853-1861.
4. Granvik, M., Vaubaillon, J., Jedicke, R. (2012). The population of natural Earth satellites. *Icarus* 218, 262-277.
5. Granvik, M., et al. (2013). Bayesian orbit-computation methods applied to temporarily-captured natural Earth satellites. In: Proc. of the Int. Symposium on Orbit Propagation and Determination (2011, Lille, France), submitted.
6. Jeffreys, H. (1946). An invariant form for the prior probability in estimation problems. Proceedings of the Royal Statistical Society London, Series A 186, 453-461.
7. Muinonen, K., Bowell, E. (1993). Asteroid orbit determination using Bayesian probabilities. Icarus 104, 255-279.
8. Muinonen, K., et al. (2012). Asteroid orbital inversion using a virtual-observation Markov-chain Monte Carlo method. Planet. Space Science Vol 73, 1, 15-20.
9. Oszkiewicz, D, Muinonen, K., Virtanen, J., Granvik, M. (2009). Asteroid ranging with Markov-chain Monte-Carlo, Meteoritics & Planetary Science, Volume 44, Issue 12, pages 1897-1904
10. Oszkiewicz, D., et al. (2012). Modeling collision probability for Earth-impactor 2008 TC3. Planet. Space Science Vol 73, 1, 30-38.
11. Virtanen, J., and Muinonen, K. (2006). Time evolution of orbital uncertainties for the impactor candidate 2004 AS1. Icarus, 184, 289-301.
12. Virtanen J., Muinonen, K., and Bowell, E. (2001). Statistical ranging of asteroid orbits. Icarus 154, 2, 412431.
13. Virtanen J., et al. (2008). Transneptunian orbit computation. In: The Solar System Beyond Neptune (A. Barucci, H. Boehnhardt, D. Cruikshank, A. Morbidelli, Eds.), pp. 25-40.